VISUAL HFLCAL – A SOFTWARE TOOL FOR LAYOUT AND OPTIMISATION OF HELIOSTAT FIELDS

Peter Schwarzbözl[1] , Mark Schmitz[2] and Robert Pitz-Paal[3]

[1] German Aerospace Centre, Solar Research, 51170 Köln, Germany, ++49 601 2967, peter.schwarzboezl@dlr.de

[2] FH Aachen, Solar-Institut Jülich, 52428 Jülich, Germany

[3] German Aerospace Centre, Solar Research, 51170 Köln, Germany

Abstract

HFLCAL is a program for layout and optimization of heliostat fields of central receiver systems (CRS) based on annual performance calculation. Computation time for performance estimation is saved by using a simplified mathematical model for the concentrator optics: the reflected image of each heliostat is described by a circular normal distribution. This approximation is justified when the standard deviation of the statistical mirror error exceeds 1 mrad. The paper shows details about the mathematical model and its validation. The HFLCAL code has been continuously used and enhanced in numerous R&D projects. The current features of HFLCAL comprise (among others) automatic multi-aiming, secondary concentrator optics, tower reflector systems, various receiver models and the ability of least-cost optimization with various optimization algorithms. A graphical user interface has been added to the program that supports menu-driven interactive commands and depicts calculation results in a display window.

Keywords: solar tower plant, central receiver system, heliostat field, modeling, simulation, optimization

1. Introduction

The computer program HFLCAL was developed by Michael Kiera at the German company Interatom during the project GAST (GAS-cooled Solar Tower) in the early 1980's ([1]). GAST was a bilateral German-Spanish cooperation aiming at the development and the investigation of necessary solar specific components and software for a gas-cooled tower power station of medium size.

The HFLCAL code was developed for two main tasks, the calculation of the annual plant output at a given configuration and the layout and optimization of a total system with respect to maximum annual electric energy yield per collector unit.

HFLCAL was acquired by the German Aerospace Centre (DLR) in 1994 and adapted it to run on current personal computers instead of a mainframe machine. Since then the program was continuously used and further developed in numerous R&D projects related to central receiver systems.

2. Mathematical Model of Solar Concentration

HFLCAL is a program for the layout of concentrator fields based on the calculation of intercepted power of a larger number of heliostats. The HFLCAL model assumes all heliostats having well canted concentrating facets of spherical curvature. The reflected image of each heliostat at a given point in time is described by one single circular normal distribution of the energy flux

$$F(r) = \frac{1}{2\pi\sigma^2} e^{-\frac{r^2}{2\sigma^2}} . \qquad \text{(Eq. 1)}$$

In reality, the size and shape of the reflected image at a given point in time is influenced by the finite size of the sun and the quality of the mirror curvature and the mirror surface. If the incident ray is not parallel to the mirror's normal, the reflected beam is further deformed by the astigmatic effect. In HFLCAL, the intercepted

energy from each heliostat over a certain period of time is of interest. Therefore, the aim-point uncertainty due to the tracking mechanism has to be considered. All these influences are aggregated into the circular normal distribution with one characteristic value σ, which can be assumed as a superposition of normal distributions:

$$\sigma^2 = \sigma_{sun}^2 + \sigma_{beam\ quality}^2 + \sigma_{astigm}^2 + (2 \cdot \sigma_{track})^2 . \quad \text{(Eq. 2)}$$

Sunshape

The solar intensity is not distributed uniformly across the sun disc but decreases towards the edge. It is often described with the Kuiper sunshape model ([3], Figure 1 left). A normal distribution with σ=2.24mrad is statistically comparable because it has the same root mean square deviation from the central ray. But the graph in figure 1 left shows a systematic overestimation of the peak at the expense of the edge. Nevertheless, the approximation of a heliostat image by a circular normal distribution is supported by the Central Limit Theorem that states that the superposition of arbitrarily distributed quantities converges towards a normal distribution. The convergence is accelerated when some of the quantities are already normally distributed.

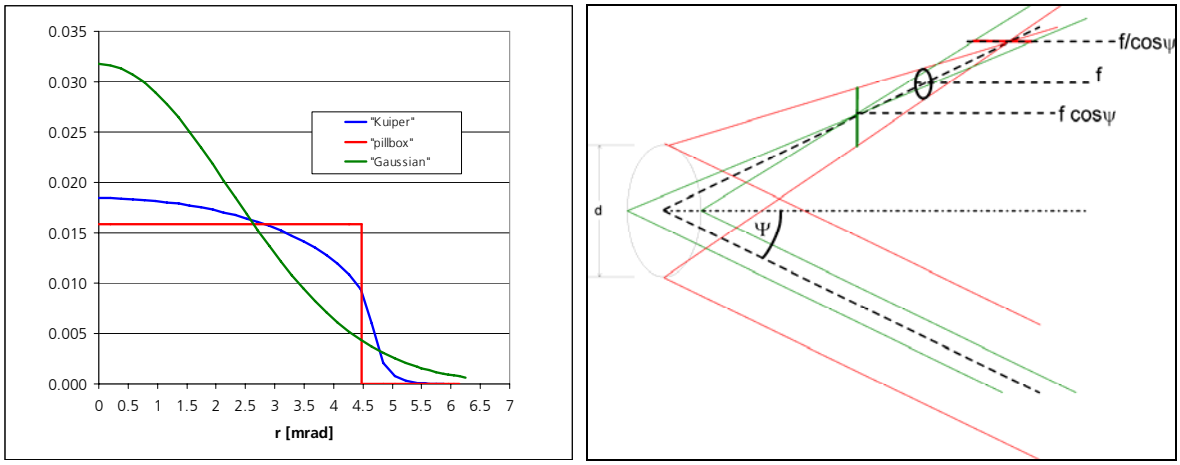

Figure 1. Left: Normalized angular distributions of solar intensity with identical root-mean-sqare (RMS) deviation from the central ray of 3.17mrad. "Kuiper" model sunshape ([3]), "Gaussian" normal distribution with σ=2.24mrad and "pillbox" distribution with radius=4.48mrad. **Right:** Off-axis-reflection of light at a spherical concentrator (Ψ: incident angle, f: focal distance of the concentrator, d: diameter of concentrator)

Beam Quality

The beam quality accounts for deviations of the mirror curvature from the ideal shape and imperfections of the reflecting surface due to waviness and roughness. These mechanisms can be measured as the so-called slope error and are described statistically by a circular normal distribution. The slope error is defined with respect to the surface normal vector; therefore its effect is doubled in the reflected ray:

$$\sigma_{beam\ quality}^2 = (2 \cdot \sigma_{slope})^2 . \qquad \text{(Eq. 3)}$$

Astigmatism

At off-axis reflection (Ψ≠0°) with a concentrator of spherical or paraboloidal shape parallel light rays are concentrated into two focal lines rather than a single focal point (Figure 1 right). For f/d >> 1, rays in the tangential plane (defined by the incoming and the reflected central ray) are concentrated in a line focus at distance f·cosΨ from the mirror, while the rays in the perpendicular sagittal plane are concentrated in a line focus f/cosΨ from the mirror. In between, at distance f, the reflected beam has minimal dimensions D= d (1-cosΨ). At an arbitrary distance SLR from the mirror the image dimensions in the tangential and sagittal plane are ([5]):

$$H_t = d \cdot \left| \frac{SLR}{f} - \cos\Psi \right|; \quad W_s = d \cdot \left| \frac{SLR}{f} \cdot \cos\Psi - 1 \right|; \quad \text{(Eq. 4)}$$

A heliostat usually consists of several facets and astigmatism occurs in the facet and in the total heliostat. In HFLCAL, each heliostat is assumed to be canted correctly for Ψ=0°. The image dimensions due to off-axis reflection are described as superposition of astigmatism in the heliostat and in the facet. The root-mean-square of the image extensions in the tangential and sagittal plane is treated as diameter of a pillbox distribution. It is incorporated into the HFLCAL image description as additional widening of the reflected beam:

$$\sigma_{astigm} = \frac{\sqrt{\tfrac{1}{2}\left(H_{t,hel+facet}^2 + W_{s,hel+facet}^2\right)}}{4 \cdot SLR} \quad ; \quad \text{(Eq. 5)}$$

Tracking

The heliostat reflecting surface is usually moved about two axes with motors and gears. Tracking errors, i.e. deviations of the mirror normal from the intended direction, are caused by the finite motor step size, tolerances of the gear boxes and wind loads on the structure. The tracking error is usually measured with respect to the mirror normal vector; therefore its effect is doubled in the reflected ray (see Eq. 2). The statistical deviations of the two tracking axes are combined into one circular symmetric distribution in HFLCAL:

$$\sigma_{track} = \sqrt{\sigma_{axis1} \cdot \sigma_{axis2}} \; . \quad \text{(Eq. 6)}$$

This is a conservative approach, valid for on-axis reflection. For off-axis reflection the influence of the tracking uncertainty is dependent on the angle between the incident ray and the axes.

Performance Calculation

When the heliostat image is described with Eq. (1), the flux distribution has to be integrated along the receiver aperture plane to get the intercepted power at a certain point in time. The intercept expressed as efficiency then reads:

$$\eta_{incp} = \frac{1}{2\pi\sigma^2} \iint_{aperture} e^{-\frac{\zeta^2+\gamma^2}{2\sigma^2}} \, d\zeta d\gamma \; ; \quad \text{(Eq. 7)}$$

The radiation power at time t from a single heliostat at location (x,y) in the field into a given aperture is then calculated as:

$$P(x,y,t) = DNI(t) \cdot F_{Mir} \cdot \eta_{refl} \cdot \eta_{atmo}(x,y) \cdot \eta_{\cos}(x,y,t) \cdot \eta_{b\&s}(x,y,t) \cdot \eta_{incp}(x,y,t) \; , \quad \text{(Eq. 8)}$$

where DNI is the direct normal solar radiation, F_{Mir} is the heliostat reflective surface, η_{refl} is the mirror reflectivity, η_{atmo} is the atmospheric attenuation depending on the distance from the receiver, η_{cos} is the cosine factor depending on heliostat and sun position and $\eta_{b\&s}$ accounts for the losses due to blocking and shadowing by the tower and neighbouring heliostats. To calculate the latter effect, a group of heliostats around each heliostat is checked geometrically for shading and blocking interferences by projecting the mirror outlines onto the planes of their neighbours.

The annual energy yield of a single heliostat is estimated as the weighted sum of power values for about 100 representative time points:

$$E_{i,annual}(x,y) = \sum_t w(t) \cdot P_i(x,y,t) \; ; \quad \text{(Eq. 9)}$$

The weighting factor *w(t)* includes the corresponding interval length and the multiplicity of each representative time point.

3. Validation

Pettit, Vittitoe and Biggs ([4]) early discussed the possibility of describing the angular distribution of reflected light from a solar concentrator with a circular normal distribution. They calculated the convolution of measured sunshapes of various widths with normally distributed mirror errors and compared the results with circular normal distributions. They found very good agreement when the mirror error was more than two times larger than the dispersion of the sun ($\sigma_{mirror} \geq 2\sigma_{sun}$).

To assess the usability of the HFLCAL model here, it was compared with ray-tracing results performed with MIRVAL ([2]). First, a single heliostat was considered consisting of 16 facets of 6m² each with 100% reflectivity. The heliostat is canted for on-axis reflection and the focal length of the facets is equal to the slant range of 141m. Figure 2 shows the results for on axis reflection of solar light with DNI of 1000 W/m². For the ray-tracing calculations a "Kuiper"-sunshape as shown in Fig. 1 was used with RMS width of 3.17mrad. Therefore, the beam dispersion for HFLCAL was set to $\sigma_{HFLCAL} = ((2.24mrad)^2 + \sigma_{beam\ quality}^2)^{1/2}$.

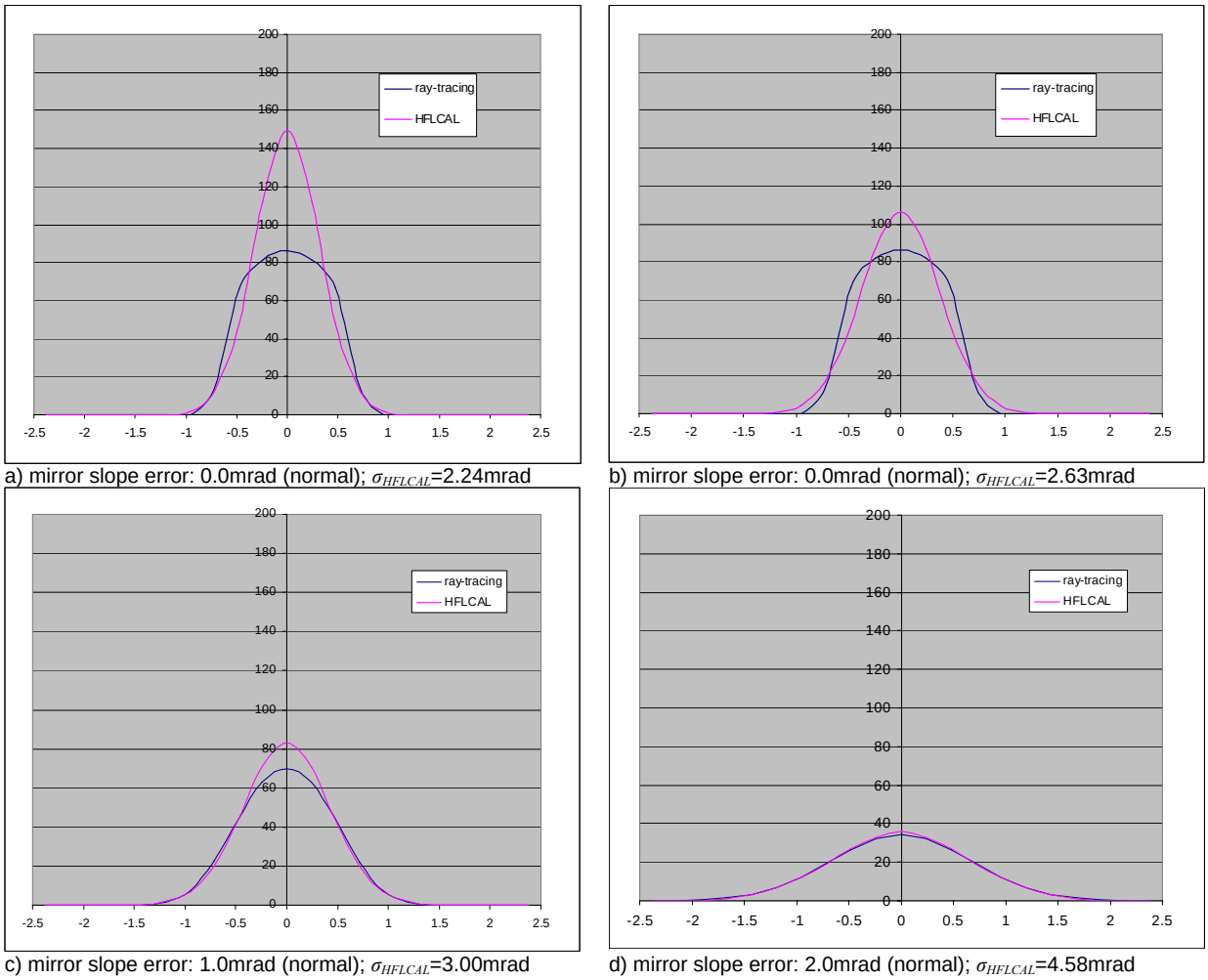

a) mirror slope error: 0.0mrad (normal); σ_{HFLCAL}=2.24mrad

b) mirror slope error: 0.0mrad (normal); σ_{HFLCAL}=2.63mrad

c) mirror slope error: 1.0mrad (normal); σ_{HFLCAL}=3.00mrad

d) mirror slope error: 2.0mrad (normal); σ_{HFLCAL}=4.58mrad

Figure 2: Flux profile of single heliostat with varying mirror beam error. Comparison of HFLCAL and MIRVAL results.

Comparing Figures 2 a), c) and d) shows, that while for small mirror errors the HFLCAL image is too narrow and has an overestimated peak flux, the deviations decrease as the mirror error increases and good agreement is reached when $\sigma_{HFLCAL} \approx 2\sigma_{sun}$. But when the root mean square deviation of the two-dimensional HFLCAL image from the ray-tracing result is considered, a minimum deviation is reached for a σ_{sun} other than 2.24mrad (Figure 2 b)).

This was repeated for various mirror errors and the results are shown in Figure 3. As can be seen, the beam dispersion for HFLCAL, σ_{HFLCAL}, (total sigma in Fig. 3 left) is converging towards 2 σ_{slope} because the influence of the solar distribution vanishes with increasing mirror errors. The RMS deviation rapidly decreases below 1% for realistic mirror slope errors >1mrad.

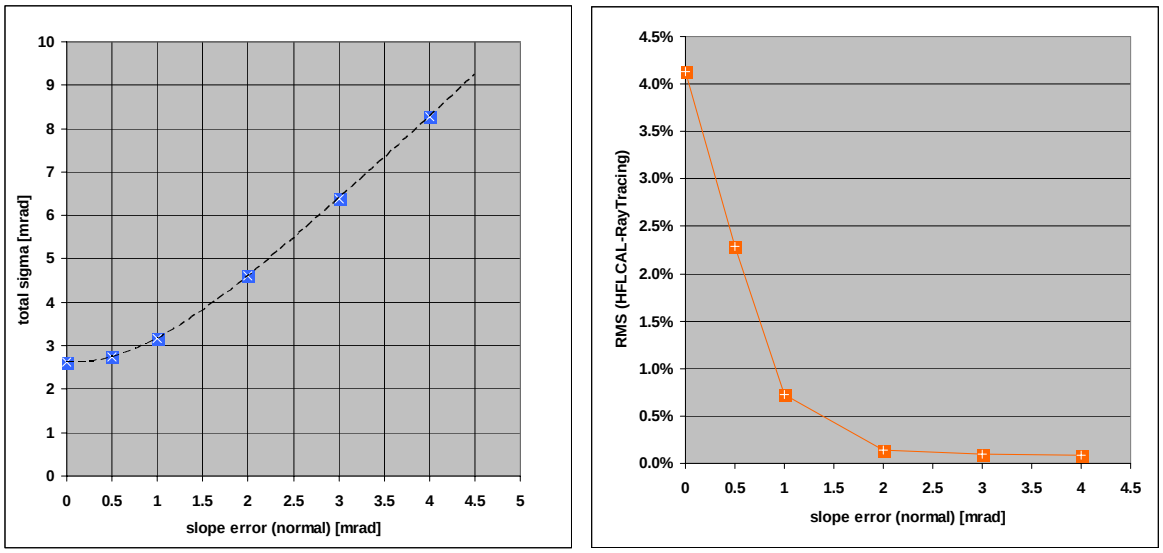

Figure 3: Best fit of HFLCAL image as a function of mirror slope error. Total sigma (left) and RMS deviation of HFLCAL image from ray-tracing result at best fit (right).

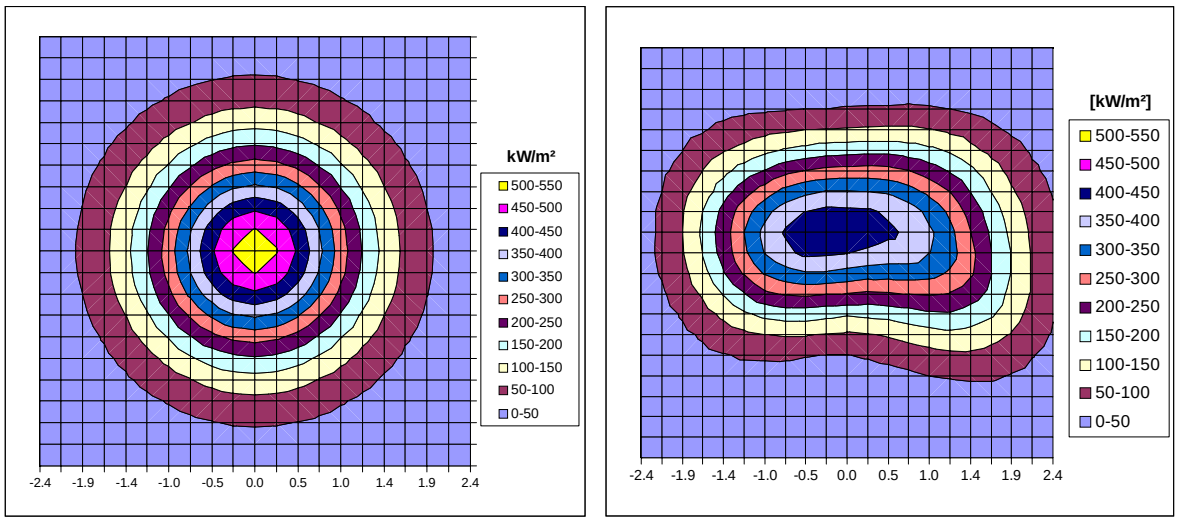

Figure 4: Flux distribution of heliostat field for average incident angle of 45° (left: HFLCAL with σ_{HFLCAL}=3.17mrad, right: MIRVAL with mirror slope error of 1mrad).

Finally, a rectangular field of 7x7 heliostats (96m² each) was considered with all heliostats aiming at the centre of the target at an average slant range of 141m². The HFLCAL distribution agreed almost perfect with the ray-tracing result. At off-axis reflection the image is distorted due to the astigmatic effect and the HFLCAL model only gives an estimate of the mean diameter of the image but it does not reproduce the correct shape due to the assumption of symmetry in Eq. 1 (see Figure 4). Nevertheless, the intercepted power differs – depending on the aperture size - only by few percent. The different mechanisms in the field are calculated as shown in Table 1.

	HFLCAL	ray-tracing (Mirval)
cosine	0.7067	0.7067
blocking & shading	0.8015	0.8086
atmospheric att.	0.9764	0.9765
interception	0.9703	0.9755
total	0.5366	0.5443

Table 1: Comparison of loss mechanisms for 7x7 heliostat field between HFLCAL and MIRVAL.

4. System Layout and Optimization

A solar tower system is configured in HFLCAL by specifying the heliostat (dimensions, beam error as in Eq. 2, reflectivity), the tower (height, radius), the receiver (shape, size, inclination, thermal efficiency) and the plant location (latitude, solar resource). The thermal receiver efficiency represents the link between the thermal losses and the optical losses of the system. A load dependent model, which is usually non-linear, is important for the correct weighting between time points.

The system layout is the determination of the required collector field size to reach the given plant design power at the design point time. Thereby, HFLCAL starts with a gross field of hypothetical heliostat positions described by a parameterized distribution, for example by linear functions of the heliostat angular and radial distance (Figure 5 left). The annual yield of intercepted energy of each heliostat in the gross field is calculated according to Eq. 9. Then the heliostats performing best on the annual basis are chosen and their design point power is added up until the desired total power can be provided (Figure 5 right). The result is a field layout with positions of single heliostats relative to the tower base.

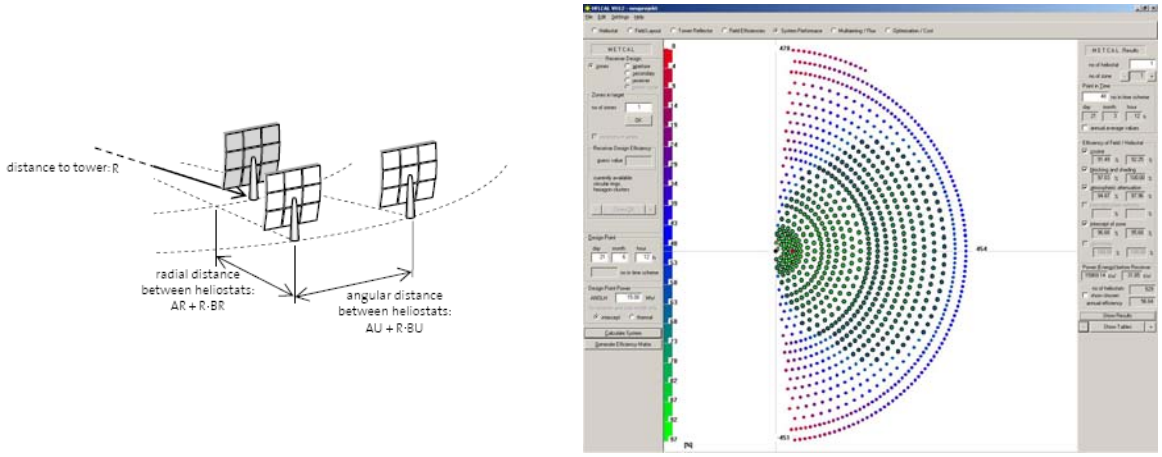

Figure 5: Left: Parameterized heliostat field setup. Right: Screenshot of Visual HFLCAL showing gross field and selected field. The colours describe the design point efficiency.

The simplified optical model of HFLCAL, as described in Chapter 2, allows performing a system layout calculation in very short computation time, usually only few seconds. Therefore it is possible to include the layout calculation in an optimization procedure. In principle, any optimization algorithm can be wrapped around the HFLCAL core to perform subsequent system layout calculations while system parameters are manipulated. Two options are currently implemented in Visual HFLCAL: Powell's Method as a direction set method for multidimensional minimization ([6]) and a genetic algorithm that maximizes the system performance by evolutionary mutation of system parameters ([7]). Best results were usually attained by combining both optimization techniques.

Additionally, cost functions can be defined to calculate the design-dependent capital investment and O&M costs for the specified solar tower system. This enables least-cost optimization of the solar part of a tower plant by minimizing the cost per MWh thermal receiver energy.

5. The Visual HFLCAL Software

While some of the core routines of HFLCAL are still in the original FORTRAN77 standard, most new features are programmed in FORTRAN95 and Visual-FORTRAN. It was decided to use Visual-FORTRAN for the user interface rather than setting up the program completely new in some other code like Visual-C++ or linking the HFLCAL code as DLL to a separate user interface. Visual-FORTRAN offers sufficient possibilities to create a windows-based graphical user interface with interactive dialogues, pop-up menus and display of results. The advantage is that all routines are combined in a single software project and handled with the same compiler. This facilitates the enhancement of the code with new features.

The Visual HFLCAL user interface allows navigating through the calculation process and provides interactive menus for all input parameters. Very valuable is the graphical system display that directly depicts definitions by the user and shows intuitive representations of the calculation results (Figure 5 right). The calculation modes comprise field layout, annual performance calculation, flux density calculation, system optimization and the creation of a field efficiency matrix to be used in other simulation tools (e.g. TRNSYS [10]).

A menu driven user interface makes it easy to change parameters but does not allow the user to change or add more complex information like model equations. Therefore, some routines were outsourced into a dynamic link library and the source code can be manipulated by the advanced user. The outsourced routines comprise the models for the thermal receiver efficiency and the models for cost calculations. Parameters for the user defined routines can be provided through the user interface of the main program.

6. Applications

HFLCAL has been used for a wide range of solar tower technologies. These include direct steam systems with cavity receiver, open volumetric air receiver with cylindrical aperture, pressurized air receiver with secondary concentrator ([8]) and beam down systems with tower reflector and secondary concentrator ([11]).

The optics of a secondary concentrator for example, was included as incident-angle-dependent transmissivity as an additional loss to the optical system (Figure 5 left). This resulted in long narrow field layouts for solar gas turbine systems with pressurized receiver. Overall system optimization was performed including single and multiple receiver clusters. (Figure 5 right, [9], [12], [13])

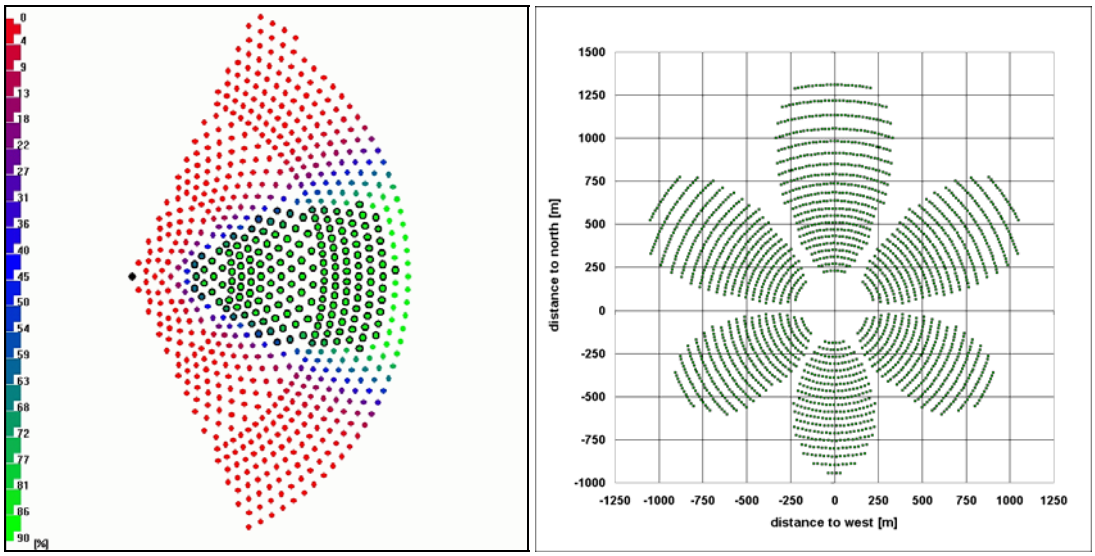

Figure 5: Left: HFLCAL-screenshot with field layout for receiver with secondary concentrator. The colours represent the secondary transmissivity. Right: Field layout for large solar gas turbine plant with six receiver clusters. Total intercept power is about 230 MW.

7. Conclusion

The HFLCAL model is suitable for the estimation of intercepted power of concentrating heliostats. It allows fast performance calculation for large heliostat fields as a basis for system layout and optimization. The HFLCAL model is not suitable for the simulation of non-concentrating or line-focusing mirrors. HFLCAL is also not suitable for the detailed analysis of flux density distributions and the corresponding receiver design. This should be done with detailed ray tracing codes.

HFLCAL shows two important features as compared to other codes. First, all calculations are based on individual heliostats and the result of a HFLCAL field layout are single heliostat positions. And second, the thermodynamic performance of the receiver can be included allowing overall system layout and optimization.

The graphical user interface of Visual HFLCAL adds the interactive usability of modern software.

References

[1] Kiera, M.: Heliostat Field: computer codes, requirements, comparison of methods. In: Becker, M., Böhmer, M. (Eds.): GAST – The Gas-Cooled Solar Tower Technology Program. Proceedings of the Final Presentation. Springer Verlag, Berlin 1989

[2] Leary, P.L., Hankins, J.D.: A User's Guide for MIRVAL - a computer code for comparing designs of heliostat-receiver optics for central receiver solar power plants. Sandia Laboratories Report, SAND77-8280, 1979

[3] Biggs, F., Vittitoe, C.: The Helios Model for the optical behaviour of reflecting solar concentrators. SANDIA report SAND78-0347. Albuquerque, USA, 1979

[4] Pettit R. B., Vittitoe C. N., Biggs F.: Simplified Calculational Procedure for Determining the Amount of Intercepted Sunlight in an Imaging Solar Concentrator. Journal of Solar Energy Engineering, Vol. 105, 1983

[5] Igel E. A., Hughes R.L.: Optical Analysis of Solar Facility Heliostats. Solar Energy, Vol. 22, 1979

[6] Press W.H., Flannery B.P., Teukolsky S.A. and Vetterling W.T.: Numerical Recipes in FORTRAN77: The Art of Scientific Computing. Cambridge University Press, 1st Edition, 1986.

[7] Carroll, D. L.: Chemical Laser Modeling with Genetic Algorithms. AIAA J., Vol. 34, 2, 1996. (General information about the genetic algorithm code used in HFLCAL can be found at www.cuaerospace.com).

[8] Buck R., Bräuning T., Denk T., Pfänder M., Schwarzbözl P. and Téllez F.: Solar-Hybrid Gas Turbine-based Power Tower Systems (REFOS). ASME Journal of Solar Energy Engineering 2002, 124: 2-9

[9] Schmitz, M., Schwarzbözl, P., Buck, R., Pitz-Paal, R.: Assessment of the potential improvement due to multiple apertures in central receiver systems with secondary concentrators. Solar Energy 80, 2006

[10] Schwarzboezl P.: A TRNSYS Model Library for Solar Thermal Electric Components (STEC). Reference Manual. Release 3.0, November 2006 (available at http://sel.me.wisc.edu/trnsys/trnlib/stec/stec.htm)

[11] Schmitz M.: Systematischer Vergleich von solarthermischen Turmreflektor- und Turmreceiversystemen. Fortschritt-Berichte VDI Reihe 6 Nr. 556, VDI Verlag, Düsseldorf 2007.

[12] Pitz-Paal, R.; Schwarzbözl, P.; Buck, R.: Solarunterstützte Gasturbinensysteme - Von der Mikrogasturbine zum GuD-Kraftkwerk. Fachverband VGB PowerTech e.V. (Ed.): VGB PowerTech, 10, 2007., S. 42 – 47

[13] Buck R., Schwarzbözl P.: Solarized Gas Turbine Power Systems. 4th International Conference "The Future of Gas Turbine Technology". 15-16 October 2008, Brussels, Belgium.